Ali, M.; Ahmed, I.; Ramirez Hoyos, P.; Nasir, S.; Cervera, J.; Mafe, S.; Niemeyer, CM.... (2017). Cesium-Induced Ionic Conduction through a Single Nanofluidic Pore Modified with Calixcrown Moieties. Langmuir. 33(36):9170-9177. doi:10.1021/acs.langmuir.7b02368

Cesium–induced ionic conduction through a single nanofluidic pore modified with calixcrown moieties

Mubarak Ali,[a,b]* Ishtiaq Ahmed,[c] Patricio Ramirez,[d] Saima Nasir,[a] Javier Cervera,[e] Salvador Mafe,[e] Christof M. Niemeyer,[c] and Wolfgang Ensinger[a]

[a]*Technische Universität Darmstadt, Fachbereich Material- u. Geowissenschaften, Fachgebiet Materialanalytik, Alarich-Weiss-Str. 2, D-64287 Darmstadt, Germany*

[b]*GSI Helmholtzzentrum für Schwerionenforschung, Planckstr. 1, D-64291 Darmstadt, Germany*

[c]*Karlsruhe Institute of Technology (KIT), Institute for Biological Interfaces (IBG-1), Hermann-von-Helmholtz-Platz, D-76344 Eggenstein-Leopoldshafen, Germany*

[d]*Departament de Física Aplicada, Universitat Politécnica de València, E-46022 València, Spain*

[e]*Departament de Física de la Tierra i Termodinàmica, Universitat de València, E-46100 Burjassot, Spain.*

* Corresponding author: E-mail address: M.Ali@gsi.de

Abstract

We demonstrate experimentally and theoretically a nanofluidic device for the selective recognition of cesium ion by exploiting host–guest interactions inside confined geometry. For this purpose, a host molecule, *i.e.*, the amine-terminated *p*-*tert*-butylcalix[4]arene-crown (*t*-BuC[4]C–NH_2), is successfully synthesized and functionalized on the surface of a single conical nanopore fabricated in polyethylene terephthalate (PET) membrane through carbodiimide coupling chemistry. On exposure to cesium cation, the *t*-BuC[4]C–Cs^+ complex is formed through host–guest interaction, leading to the generation of positive fixed charges on the pore surface. The asymmetrical distribution of these groups along the conical nanopore leads to the

electrical rectification observed in the current–voltage (*I–V*) curve. On the contrary, other alkali cations are not able to induce any significant change in the rectification characteristics of the nanopore. The success of the chemical modification is monitored from the changes in the electrical readout of the nanopore. Theoretical results based on the Nernst-Planck and Poisson equations demonstrate further the validity of the experimental approach to the cesium-induced ionic conduction of the nanopore.

Keywords: synthetic nanopores; host–guest interactions; calixcrown; current rectification; surface modification; track-etching.

1. Introduction

Metal ions in biological systems take part in a variety of essential processes and some of these ions can cause adverse effects. In particular, cesium ion is linked to negative health effects in its radioactive form.[1,2] Cesium has some similarities with potassium and then it can be easily imported in the cellular matrix through membrane transport mechanisms, causing serious health problems.[3-5] Previously, cesium detection in environmental and biological samples has been achieved through electrochemical and optical sensors,[6,7] ion exchange,[8] atomic absorption spectroscopy [9] and mass spectrometry techniques.[10]

Recently, much attention has been paid to the synthesis of a variety of macrocyclic molecules such as crown ethers, crytophanes and calixarenes for the detection of metal ions based on host-guest complexation.[6,7,11-14] Among the various supramolecular compounds, calixarene are frequently used in ionic recognition and separation processes. The phenolic moieties in calixarene can be functionalized with a variety of chemical groups to miniaturise ion selective receptors. Particularly, calix[4]arene-crown derivatives in 1,3-alternate conformation are considered as highly efficient cesium complexing agents.[11-14] In this conformation, the cesium ion is coordinated with the oxygen atoms of the crown ether and interact also with the π-electrons of the two aromatic rings in the calixarene unit.[14] This property of calixcrown derivatives finds application in the selective removal of radio-active cesium (^{137}Cs) from nuclear wastes.[15,16]

For practical applications, calixcrown moieties should be properly organized on suitable surfaces.[17-19] To this end, Zhang and Echegoyen have arranged the self-assembled layer (SAM) of two conformational isomers of thiol-terminated *p-tert*-butylcalix[4]crown on gold surface. They have demonstrated that the 1,3-alternate

isomer exhibits remarkable binding capability towards Cs^+ ion.[19] Similarly, Britt and co-workers have also demonstrated a SAM coated microcantilever functionalized with 1,3-alternate calix[4]benzocrown for Cs^+ ion recognition.[17] Recently, Yi *et al*. studied stimuli-responsive microspheres having calixcrown moieties for the selective removal of Cs^+ ion from seawater.[18] Mori and co-workers have also studied the Cs^+ ion selectivity of various conformations of calixcrown moieties using liquid membrane electrodes.[12] However, the design and development of a nanofluidic pore allowing for Cs^+ sensing is still a challenge.

In living organisms, ion channels regulate the flow of ions across the cell membrane to facilitate the electrochemical communication with the extracellular environment.[20] Ion channels with defined interfacial chemistry display gating and current rectification phenomena because of their ability to selectively transport a specific ion.[20-22] Ionic conduction is also regulated through environmental stimuli.[21,22] The ion channels can be in the open or closed states in response to external stimuli. Moreover, these channels have proved useful for a variety of applications in nanobiotechnology such as sensing and manipulation of single molecules.[23-25] Inspired from the functionality of ion channels, various routes have been proposed to fabricate synthetic nanopores in insulating solid-state materials.[26-28] Alternatively, the nanopore fabrication using ion track technology allows also to control the shape, size, and surface properties on demand.[29-36] These nanopore have already been functionalized with metal chelating ligands to miniaturise electrochemical devices for the detection of different metal cations.[30,37-43] Moreover, the nanopore surface has also been decorated with a variety of host molecules for the binding of guest analytes through host-guest inteactions.[44-51] To the best of our knowledge, however, Cs^+ ion detection using a nanofluidic pore has not yet been explored.

We demonstrate here cesium-induced ionic conduction using a nanofluidic diode based on a single asymmetric nanopore decorated with calixcrown moieties. To this end, we have designed and synthesized the amine-terminated *p-tert*-butylcalix[4]arene-crown (*t*-BuC[4]C–NH_2) molecule (Figure 1). The calixcrown molecules are then functionalized on the nanopore walls by using carbodiimide coupling chemistry. On exposure to the cesium cation in the external solution, the *t*-BuC[4]C–Cs^+ complex is formed which imparts positive charge to the pore surface. This fact leads to selective transport of ions through the nanopore. On the contrary, other alkali cations do not induce any significant change in the rectification characteristics of the nanopore. The confirmation of the chemical modification is achieved via the changes in the rectified ion current observed in the current–voltage (*I–V*) characteristics prior to and after the nanopore functionalization.

2. Materials and methods

2.1 Materials

All the chemicals and solvents, including *N*-(3-dimethylaminopropyl)-*N*′-ethylcarbodiimide·HCl (EDC·HCl), pentafluorophenol (PFP), 5(6)-carboxyfluorescein (Fcn), *N*-Boc-1,6-hexanediamine, *N*,*N*-diisopropylethylamine (DIPEA), *p-tert*-butylcalix[4]arene (*t*BuC[4]), pentaethylene glycol ditosylate, potassium *t*-butoxide (*t*-BuOK), potassium carbonate, chloroacetyl chloride, cesium carbonate (Cs_2CO_3), potassium iodide (KI), trifluoroacetic acid (TFA), lithium chloride (LiCl), sodium chloride, (NaCl), potassium chloride (KCl), rubidium chloride (RbCl) and cesium chloride (CsCl) were purchased from Sigma-Aldrich, Taufkirchen, Germany, and used without further purification.

^{1}H and ^{13}C NMR spectra were recorded at 500 and 125 MHz in $CDCl_3$, respectively. High-resolution mass spectra were measured using a Finnigan MAT90 mass spectrometer. Analytical TLC (silica gel, 60F-54, Merck) and spots were visualized under UV light and/or phosphomolybdic acid-ethanol. Flash column chromatography was performed with silica gel 60 (70-230 mesh, Merck) and basic aluminum oxide (activated, basic, ~150 mesh, 58 Å, Aldrich).

2.2 Fabrication of single asymmetric nanopores

Asymmetric track-etching technique was employed to fabricate single conical nanopores in polyethylene terephthalate (PET) membranes.[29] The first step was the irradiation of 12 μm thick PET foils (Hostaphan RN 12, Hoechst) with single swift heavy ions (Au) of kinetic energy 11.4 MeV/nucleon at the linear accelerator UNILAC (GSI Helmholtz Centre for Heavy Ion Research, Darmstadt, Germany). Secondly, the latent ion tracks of the swift heavy ion in polymer membranes were sensitized with soft UV light. Finally, the chemical track-etching process was performed in a custom-made conductivity cell having three chambers. This conductivity cell was employed for the simultaneous fabrication of the single-pore and multipore membranes. To achieve this goal, a single-shot (1 ion hitting the foil) membrane and a membrane irradiated with 10^7 ions per cm^2 were placed on the sides of the middle compartment of the conductivity cell and clamped tightly. An etching solution (9 M NaOH) was filled in the middle compartment having apertures on both sides. In this way, the chemical etchant was in direct contact with both membranes. The two compartments on either side of the middle chamber were filled with a stopping solution (1 M KCl + 1 M HCOOH). To monitor the etching process, gold electrodes were inserted on both sides of the single-ion irradiated membrane and a potential of –1 V was applied across the membrane. The etching process was carried

out at room temperature. The current remained zero as long as the etchant had not permeated the whole length of the membrane. After the breakthrough (a point at which the etchant pierced the membrane), an increase in the ionic current through the nascent pore was observed. The etching process was stopped when the current reached a certain defined value. Then, the membranes were thoroughly washed with stopping solution in order to neutralise the etchant, followed by deionized water. The etched membranes were then dipped in deionized water overnight in order to remove the residual salts. This process resulted in polymer samples containing approximately conical single pores with the carboxylic groups (COOH) generated on the inner pore walls due to the hydrolysis of ester bonds in the back-bone of polymer chains.

2.3 Synthesis of *t*-BuC[4]C–NH_2 (6)

Figure 1 depicts the preparation of the different calixcrown ether derivatives involved in the synthesis of amine-terminated p-tert-butylcalix[4]arene-crown (**6**) by following previously reported reaction procedures with slight modifications.[19,52,53] Details of the synthesis are given in the Electronic Supplementary Information (ESI) file.

Briefly, we have synthesized amine-terminated *p-tert*-butylcalix[4]arene-crown (*t*-BuC[4]C–NH_2) to modulate the nanopore surface chemistry and transport properties in response to cesium cation. The reaction scheme for the synthesis of *t*-BuC[4]C–NH_2 is shown in Figure 1. Commercially available *p-tert*-butylcalix[4]arene (**1**) and pentaethylene glycol ditosylate (**2**) were treated with potassium *tert*-butoxide in dry benzene to afford calixcrown ether derivative **(3)** according to an established method.[52] Chloroacetamide **(4)** was synthesized by adopting a previously reported procedure.[53] Then, chloroacetamide **(4)** and calixcrown **(3)** were refluxed in the presence of cesium carbonate with the a catalytic amount of potassium iodide to

afford Boc-protected amine, *i.e.*, *t*-BuC[4]C–NHBoc **(5)**.[19] Deprotection was carried out using trifluoroacetic acid to afford *t*-BuC[4]C–NH_2 (**6**) which was used without further purification in the nanopore modification reaction. The chemical structures of calixcrown ether derivatives were characterized through 1H NMR, 13CNMR and HRMS-FAB techniques.

2.4 Chemical functionalization of nanopore surface

The chemical etching led to the generation of the carboxylic acid (–COOH) groups on the pore surface. These groups exposed were first converted into amine-reactive esters through carbodiimide coupling chemistry. To this end, the track-etched single-pore membrane was immersed in an ethanol solution containing EDC (100 mM) and PFP (200 mM) at room temperature. The activation process was carried out for 1 h. The membrane was washed with ethanol several times. Then, the activated pore was dipped in *t*-BuC[4]C–NH_2 (12 mM) solution prepared in anhydrous ethanol for 15 h. During this reaction period, amine-reactive PFP-esters were covalently coupled with terminal amine group of the *t*-BuC[4]C–NH_2. Subsequently, the modified pore was washed thoroughly with ethanol followed by careful rinsing with deionized water.

2.5 Contact angle measurements

For contact angle analysis, native PET foil without heavy ion irradiation was used. To prepare the samples for the contact angle (CA) measurements, the PET foil was exposed to an etchant solution for 55 min. After washing with water, the PET foil was dipped in the stopping solution for 2 h. The sample was then exposed to deionized water overnight. The wetting properties (contact angle) of unmodified and *t*-BuC[4]C-modified surfaces were measured using a contact angle measurement setup equipped

with a side camera (IDS uEye camera) and a goniometer. To measure the respective contact angle, 5 microliter of water was dropped on the foil using a micropipette.

2.6 Current-voltage measurements

The unmodified and modified pores were characterized by measuring the current–voltage (*I–V*) curves before and after functionalization. The electrolyte solutions were prepared in 10 mM tris-buffer (pH 6.5). The measurement of *I–V* curve was performed using a picoammeter/voltage source (Keithley 6487, Keithley Instruments, Cleveland, Ohio, USA) using LabVIEW 6.1 (National Instruments). For this purpose, the single-pore (as-prepared) membrane was fixed between the two compartments of the conductivity cell. An aqueous electrolyte was filled in both halves of the cell. The electrodes having a Ag wire coated with AgCl were inserted into each half-cell solution to establish a transmembrane potential difference (voltage) and the ionic current through the pore was then measured. For the case of the conical nanopore, the ground and working electrodes were placed on the base and tip side of the pore, respectively. In order to record the *I–V* curves, a scanning triangle voltage signal from –2 to +2 V was used.

2.7 Modeling

The experimental *I–V* curves were described using a theoretical model based on the Poisson and Nernst-Planck (PNP) equations.[54-57] This simplified, one dimensional model assumes a conical geometry for the nanopore and gives the *I–V* curves in terms of the tip (*d*) and base (*D*) diameters of the pore and the surface concentration σ of fixed charges. For the sake of simplicity, this surface concentration was assumed to be constant along the pore length (see further details in the supporting information).

3. Results and discussion

Figure 2 shows *I–V* curves of the as-prepared (before modification) single nanopore measured in 100 mM KCl solution at neutral and acidic conditions. To achive this goal, the single-pore membrane was fixed between the two chambers of the conductivity cell. The electrolyte solution was filled on both sides of the single pore membrane and the electrodes on each side of the nanopore were arranged in such a way that high currents at positive voltages and low currents at negative voltages were obtained. Experimental and theoretical[54-59] studies have proved that the as-prepared single conical pores exhibit cation-selectivity and rectify the ion current (*i.e.*, cations preferentially flow from the tip towards the base opening) due to presence of ionized $–COO^-$ groups on the pore surface at neutral pH conditions.

The base opening (*D*) diameter of the conical pore was directly calculated from the field emission scanning electron microscopy images of the multipore membrane simultaneously etched with the single-pore foil (Figure 3C). The pore tip (*d*) opening was calculated from the linear fitting of the *I–V* curve for the uncharged nanopore (σ = 0) at pH 3.5 (Figure 2). In our case, D = 270 nm, d = 20 nm and the membrane thickness L = 12 μm. Once the pore diameters were determined, the only free parameter of the model was the surface charge density that was calculated from the fitting of the *I–V* curve of the as-synthesized pore at pH 6.5 to the theoretical model. The best fitting was obtained for σ = -0.2 e/nm^2, where e is the elementary charge (Figure 2).

Figure 3A shows the immobilization of *t*-BuC[4]C–NH_2 molecules on the nanopore surface. For this purpose, the (–COOH groups were first activated by exposing the single-pore membrane to a solution of EDC and pentafluorophenol (PFP). This step resulted in the formation of an amine-reactive PFP reactive-ester

on the pore surface. Then, the activated single-pore membrane was exposed to a *t*-BuC[4]C–NH_2 solution. During this reaction step, the PFP-reactive intermediate was covalently coupled with the terminal-amine groups of *t*-BuC[4]C molecules.

To verify the success of the chemical reaction, the wetting properties of PET foil were studied by CA measurements before and after modification. The PET foil was treated using the same experimental protocol as the single-pore membrane. Figure 3B shows the contact angle of the PET foil having carboxylic acid groups (54 ± 2)°. After the functionalization of *t*-BuC[4]C moieties, the contact angle increases to 83 ± 2°. This result suggests that the modified PET surface becomes more hydrophobic due to the presence of tertiarybutyl group *t*-BuC[4]C moieties.

Previous studies have demonstrated that calixcrowns (host) in 1,3-alternate conformation exhibit remarkable affinity towards Cs^+ ion (guest).[17-19] The host-guest complexation occuring inside the confined environment is used to tune the pore surface charge density and ionic conduction. Figure 4A represents the Cs^+ ion complexation with *t*-BuC[4]C moieties on the nanopore surface via coordination with crown ether oxygen atoms and cation–π interactions originated from the aromatic rings of 1,3-alternate conformation.[14]

Figure 4B shows the *I–V* characteristics of the single conical pore decorated with *t*-BuC[4]C moieties in the presence of various cesium concentrations prepared in 10 mM Tris-buffer (pH 6.5). At low Cs^+ concentration (≤ 1 mM), the *t*-BuC[4]C-modified pore was in a nonconducting "*off*" state, as observed from the very low current (~ 0.2 nA) flowing across the membrane. When the modified pore was exposed to 10 mM and 25 mM Cs^+ concentrations, the rectified current at –2 V increases from 0.2 to 0.4 nA and 0.7 nA, respectively. This fact suggests that the Cs^+ ion makes the pore selective to anions due to the formation of a positively

charged complex between the *t*-BuC[4]C moities and the metal cation on the pore surface. By further increasing the Cs^+ ion concentration from 25 mM to 100 mM, the rectified ion current increases from 0.7 nA to 1.66 nA at –2 V. No significant change in the positive current at +2 V was observed on exposing the modified pore to various Cs^+ concentrations. This fact clearly shows that *t*-BuC[4]C–Cs^+ complexes switched the pore transport behaviour from the nonconducting "*off*" state to conducting "*on*" state. Moreover, the Cs^+ concentrations affect the extent of anion conduction across the modified single-pore membrane. The continuous curves of Figure 4B show the model results assuming that the complexation of Cs^+ ions produces a positive fixed charge density on the pore surface. These curves have been calculated using the same charge density $\sigma = 0.05\ e/nm^2$ for all the Cs^+ concentrations. The presence of the Cs^+ ions can reverse the pore charge even at low concentrations. The qualitative agreement between theory and experiment for $V < 0$ suggests that the substitution of the carboxylic acid groups of the as-prepared pore with the tert-butylcalix[4]arene–crown (t-BuC[4]C) moieties is significant. For $V > 0$ the model overstimates the currents, probably due to a spatial accumulation of positive fixed charges close to the pore tip (see reference 54 for details).

We proceeded now to study the specificity of the *t*-BuC[4]C–modified pore towards various alkali cations. To this end, the same modified pore was exposed to electrolyte solutions having different alkali ions at 100 mM and pH 6.5. The *I–V* curves of Figure 4C did not show any significant change in the rectified current in response to Li^+, Na^+, K^+, and Rb^+ cations. On the contrary, upon exposure to Cs^+ ion, the pore exhibited high ionic current rectification (Figure 4C). This fact suggests that the functional calixcrown moieties have the ability to specifically bind

the Cs^+ cation. The *t*-BuC[4]C–Cs^+ complex imparts positive charge to the pore surface, leading to current rectification. This fact shows that the inner pore was switched from a hydrophobic and uncharged non-conductive state to a hydrophilic and charged conductive state upon exposure to Cs^+ ion. This result is in agreement with the model calculations shown in Figure 4C, where the curve corresponding to CsCl was calculated using σ = 0.05 e/nm^2. In the case of the other alkali cations, the estimated σ value was very low (~ 0.005 e/nm^2). Again, the deviations between theory and experiments for $V > 0$ should be ascribed to an accumulation of positive fixed charges close to the pore tip.[54]

Figure 5A shows the pore conductance as a function of the Cs^+ concentration and the type of alkali cation. The data is obtained from the respective *I–V* curves of Figure 4B and 4C at –2 V. Increasing the Cs^+ concentration led to a gradual increase in the pore conductance because of the positive charges originated by the binding of Cs^+ cations to calixcrown moieties. For the case of other alkali cations, the small increases in the conductance were noticed on exposure to Li^+ and Na^+ cation solutions. While the pore exhibits some conductance on exposing to K^+ and Rb^+ solutions, suggesting the partial complexation of these cations with the calixcrown moieties, the sharp increase in the Cs^+ conductance with respect to the case of the other alkali cations confirms the specific binding of this cation. Figure 5B shows the variation of current over different cycles of reversible binding and unbinding of the Cs^+ ions in the absence and presence of this ion. The reversible changes observed in the ion current suggest again that the surface charge density dictates the transport properties, switching the nanopore from a nonconducting state with calixcrown moieties to a conducting state with *t*-BuC[4]C–Cs^+ chelates.

Finally, we have also examined the reproducibility of the nanofluidic device. To this end, we have fabricated another single conical nanopore. In this case, we have also performed the control measurements using a non-functionalized nanopore. Figure 6A shows *I–V* curves of the as-prepared single nanopore before modification measured in 100 mM alkali electrolyte solutions. Then the conical nanopore was functionalized with calixcrown moieties under the same set of experimental conditions. Figure 6B shows that addition of Li^+, Na^+, K^+ and Rb^+ cations in the electolyte solution caused relatively small changes in the current. On the contrary, exposure to Cs^+ ion led to a significant change in the *I–V* behavior: current rectification was observed due to the formation of *t*-BuC[4]C–Cs^+ complexes, enabling anion conduction through the modified nanopore.

4. Conclusions

In summary, we have described experimentally and theoretically Cs^+ ion induced ion conduction through a nanofluidic pore functionalized with calixcrown moieties via carbodiimide coupling chemistry. On exposure to Cs^+ ion, the asymmetrical distribution of positively charged groups along the conical nanopore led to the selective conduction of anions, resulting in the inversion of the rectification observed in the *I–V* curve. On the contrary, other alkali cations did not show drastic changes in the current rectification. Theoretical modelling of the experimental results based on the Nernst-Planck and Poisson equations confirmed further the validity of the experimental approach to cesium-induced ion conduction through single nanofluidic pores.

Acknowledgements

M.A., S.N. and W.E. acknowledge the funding from the Hessen State Ministry of Higher Education, Research and the Arts, Germany, under the LOEWE project iNAPO. P.R., J.C. and S.M. acknowledge financial support by the Spanish Ministry of Economic Affairs and Competitiveness (MAT2015-65011-P), and FEDER. I.A. and C.M.N. acknowledge financial support through the Helmholtz programme BioInterfaces in Technology and Medicine. The authors are thankful to Prof. Christina Trautmann from GSI (Department of Material Research) for support with the heavy ion irradiation experiments and Dr. M. Nawaz Tahir (Johannes Gutenberg University Mainz) for help in contact angle measurements.

References

(1) Rahman, M. M.; Voigt, G. Radiocaesium soil-to-plant transfer in tropical environments. *J. Environ. Radioact.* **2004**, *71*, 127-138.

(2) Rowan, D. J.; Rasmussen, J. B. Bioaccumulation of Radiocesium by Fish: the Influence of Physicochemical Factors and Trophic Structure. *Can. J. Fish. Aquat. Sci.* **1994**, *51*, 2388-2410.

(3) Cecchi, X.; Wolff, D.; Alvarez, O.; Latorre, R. Mechanisms of Cs+ blockade in a Ca2+-activated K+ channel from smooth muscle. *Biophys. J.* **1987**, *52*, 707-716.

(4) Davis, D. G.; Murphy, E.; London, R. E. Uptake of cesium ions by human erythrocytes and perfused rat heart: a cesium-133 NMR study. *Biochemistry* **1988**, *27*, 3547-3551.

(5) Ehmann, W. D.; Markesbery, W. R.; Alauddin, M. Brain trace elements in Alzheimer's disease. *Neurotoxicology* **1986**, *7*, 197-206.

(6) Joseph, R.; Rao, C. P. Ion and Molecular Recognition by Lower Rim 1,3-Di-conjugates of Calix[4]arene as Receptors. *Chem. Rev.* **2011**, *111*, 4658-4702.

(7) Kumar, N.; Leray, I.; Depauw, A. Chemically derived optical sensors for the detection of cesium ions. *Coord. Chem. Rev.* **2016**, *310*, 1-15.

(8) Sun, B.; Hao, X.-G.; Wang, Z.-D.; Guan, G.-Q.; Zhang, Z.-L.; Li, Y.-B.; Liu, S.-B. Separation of low concentration of cesium ion from wastewater by electrochemically switched ion exchange method: Experimental adsorption kinetics analysis. *J. Hazard. Mater.* **2012**, *233–234*, 177-183.

(9) Groll, H.; Schnürer-Patschan, C.; Kuritsyni, Y.; Niemax, K. Wavelength modulation diode laser atomic absorption spectrometry in analytical flames. *Spectrochim. Acta B: At. Spectrosc.* **1994**, *49*, 1463-1472.

(10) Liezers, M.; Farmer, O. T.; Thomas, M. L. Low level detection of 135Cs and 137Cs in environmental samples by ICP-MS. *J. Radioanal. Nucl.Chem.* **2009**, *282*, 309.

(11) Asfari, Z.; Bressot, C.; Vicens, J.; Hill, C.; Dozol, J.-F.; Rouquette, H.; Eymard, S.; Lamare, V.; Tournois, B. Doubly Crowned Calix[4]arenes in the 1,3-Alternate Conformation as Cesium-Selective Carriers in Supported Liquid Membranes. *Anal. Chem.* **1995**, *67*, 3133-3139.

(12) Bocchi, C.; Careri, M.; Casnati, A.; Mori, G. Selectivity of Calix[4]arene-crown-6 for Cesium Ion in Ise: Effect of the Conformation. *Anal. Chem.* **1995**, *67*, 4234-4238.

(13) Casnati, A.; Pochini, A.; Ungaro, R.; Ugozzoli, F.; Arnaud, F.; Fanni, S.; Schwing, M.-J.; Egberink, R. J. M.; de Jong, F.; Reinhoudt, D. N. Synthesis, Complexation, and Membrane Transport Studies of 1,3-Alternate Calix[4]arene-crown-6 Conformers: A New Class of Cesium Selective Ionophores. *J. Am. Chem. Soc.* **1995**, *117*, 2767-2777.

(14) Ungaro, R.; Casnati, A.; Ugozzoli, F.; Pochini, A.; Dozol, J.-F.; Hill, C.; Rouquette, H. 1,3-Dialkoxycalix[4]arenecrowns-6 in 1,3-Alternate Conformation: Cesium-Selective Ligands that Exploit Cation-Arene Interactions. *Angew. Chem. Int. Ed.* **1994**, *33*, 1506-1509.

(15) Dozol, J. F.; Casas i Garcia, J.; Sastre, A. M.: Application of Crown-Ethers to Caesium and Strontium Removal from Marcoule Reprocessing Concentrate. In *New Separation Chemistry Techniques for Radioactive Waste and Other Specific Applications*; Cecille, M. L., Casarci, M., Pietrelli, L., Eds.; Springer Netherlands: Dordrecht, 1991; pp 173-185.

(16) Dozol, M.: Possible Applications of Crown-Ethers to Metal Extraction Using Liquid Membrane Technology A Literature Survey. In *New Separation Chemistry Techniques for Radioactive Waste and Other Specific Applications*; Cecille, M. L., Casarci, M., Pietrelli, L., Eds.; Springer Netherlands: Dordrecht, 1991; pp 163-172.

(17) Ji, H.-F.; Finot, E.; Dabestani, R.; Thundat, T.; Brown, G. M.; Britt, P. F. A novel self-assembled monolayer (SAM) coated microcantilever for low level caesium detection. *Chem. Commun.* **2000**, 457-458.

(18) Yi, R.; Ye, G.; Lv, D.; Chen, J. Novel thermo-responsive hydrogel microspheres with calixcrown host molecules as cross-links for highly specific binding and controllable release of cesium. *RSC Adv.* **2015**, *5*, 55277-55284.

(19) Zhang, S.; Echegoyen, L. Self-assembled monolayers of different conformers of p-tert-butylcalix[4]crown-6 derivatives and their metal cation recognition properties. *Tetrahedron Lett.* **2003**, *44*, 9079-9082.

(20) Hille, B.: *Ionic channels of excitable membranes*; 3rd ed.; Sinauer Associates Inc.: Sunderland, MA, 2001.

(21) Doupnik, C. A.; Davidson, N.; Lester, H. A. The inward rectifier potassium channel family. *Curr. Opin. Neurobiol.* **1995**, *5*, 268-277.

(22) MacKinnon, R. Potassium Channels and the Atomic Basis of Selective Ion Conduction (Nobel Lecture). *Angew. Chem. Int. Ed.* **2004**, *43*, 4265-4277.

(23) Bayley, H.; Cremer, P. S. Stochastic sensors inspired by biology. *Nature* **2001**, *413*, 226-230.

(24) Healy, K. Nanopore-based single-molecule DNA analysis. *Nanomedicine* **2007**, *2*, 459-481.

(25) Howorka, S.; Siwy, Z. Nanopore analytics: sensing of single molecules. *Chem. Soc. Rev.* **2009**, *38*, 2360-2384.

(26) Dekker, C. Solid-state nanopores. *Nat. Nanotechnol.* **2007**, *2*, 209-215.

(27) Hou, X.; Guo, W.; Jiang, L. Biomimetic smart nanopores and nanochannels. *Chem. Soc. Rev.* **2011**, *40*, 2385-2401.

(28) Siwy, Z. S.; Howorka, S. Engineered voltage-responsive nanopores. *Chem. Soc. Rev.* **2010**, *39*, 1115-1132.

(29) Apel, P. Y.; Korchev, Y. E.; Siwy, Z.; Spohr, R.; Yoshida, M. Diode-Like Single-Ion Track Membrane Prepared by Electro-Stopping. *Nucl. Instrum. Methods Phys. Res., Sect. B* **2001**, *184*, 337-346.

(30) Ali, M.; Nasir, S.; Ramirez, P.; Cervera, J.; Mafe, S.; Ensinger, W. Calcium Binding and Ionic Conduction in Single Conical Nanopores with Polyacid Chains: Model and Experiments. *ACS Nano* **2012**, *6*, 9247-9257.

(31) Ali, M.; Ramirez, P.; Nguyen, H. Q.; Nasir, S.; Cervera, J.; Mafe, S.; Ensinger, W. Single Cigar-Shaped Nanopores Functionalized with Amphoteric Amino Acid Chains: Experimental and Theoretical Characterization. *ACS Nano* **2012**, *6*, 3631-3640.

(32) Gyurcsanyi, R. E. Chemically-modified nanopores for sensing. *Trends Anal. Chem.* **2008**, *27*, 627-639.

(33) Lepoitevin, M.; Nguyen, G.; Bechelany, M.; Balanzat, E.; Janot, J.-M.; Balme, S. Combining a sensor and a pH-gated nanopore based on an avidin-biotin system. *Chem. Commun.* **2015**, *51*, 5994-5997.

(34) Wen, L.; Tian, Y.; Ma, J.; Zhai, J.; Jiang, L. Construction of biomimetic smart nanochannels with polymer membranes and application in energy conversion systems. *Phys. Chem. Chem. Phys.* **2012**, *14*, 4027-4042.

(35) Zhang, H.; Hou, X.; Zeng, L.; Yang, F.; Li, L.; Yan, D.; Tian, Y.; Jiang, L. Bioinspired Artificial Single Ion Pump. *J. Am. Chem. Soc.* **2013**, *135*, 16102-16110.

(36) Zhang, H.; Tian, Y.; Jiang, L. From symmetric to asymmetric design of bio-inspired smart single nanochannels. *Chem. Commun.* **2013**, *49*, 10048-10063.

(37) Ali, M.; Ahmed, I.; Ramirez, P.; Nasir, S.; Niemeyer, C. M.; Mafe, S.; Ensinger, W. Label-Free Pyrophosphate Recognition with Functionalized Asymmetric Nanopores. *Small* **2016**, *12*, 2014-2021.

(38) Ali, M.; Nasir, S.; Nguyen, Q. H.; Sahoo, J. K.; Tahir, M. N.; Tremel, W.; Ensinger, W. Metal Ion Affinity-based Biomolecular Recognition and Conjugation inside Synthetic Polymer Nanopores Modified with Iron-Terpyridine Complexes. *J. Am. Chem. Soc.* **2011**, *133*, 17307-17314.

(39) Ali, M.; Ramirez, P.; Duznovic, I.; Nasir, S.; Mafe, S.; Ensinger, W. Label-free histamine detection with nanofluidic diodes through metal ion displacement mechanism. *Colloids Surf., B* **2017**, *150*, 201-208.

(40) Han, C.; Su, H.; Sun, Z.; Wen, L.; Tian, D.; Xu, K.; Hu, J.; Wang, A.; Li, H.; Jiang, L. Biomimetic Ion Nanochannels as a Highly Selective Sequential Sensor for Zinc Ions Followed by Phosphate Anions. *Chem. Eur. J.* **2013**, *19*, 9388-9395.

(41) Liu, Q.; Xiao, K.; Wen, L.; Lu, H.; Liu, Y.; Kong, X.-Y.; Xie, G.; Zhang, Z.; Bo, Z.; Jiang, L. Engineered Ionic Gates for Ion Conduction Based on Sodium and Potassium Activated Nanochannels. *J. Am. Chem. Soc.* **2015**, *137*, 11976-11983.

(42) Perez-Mitta, G.; Albesa, A. G.; Knoll, W.; Trautmann, C.; Toimil-Molares, M. E.; Azzaroni, O. Host-guest supramolecular chemistry in solid-state nanopores: potassium-driven modulation of ionic transport in nanofluidic diodes. *Nanoscale* **2015**, *7*, 15594-15598.

(43) Tian, Y.; Hou, X.; Wen, L. P.; Guo, W.; Song, Y. L.; Sun, H. Z.; Wang, Y. G.; Jiang, L.; Zhu, D. B. A biomimetic zinc activated ion channel. *Chem. Commun.* **2010**, *46*, 1682-1684.

(44) Liu, Q.; Wen, L.; Xiao, K.; Lu, H.; Zhang, Z.; Xie, G.; Kong, X.-Y.; Bo, Z.; Jiang, L. A Biomimetic Voltage-Gated Chloride Nanochannel. *Adv. Mater.* **2016**, *28*, 3181-3186.

(45) Liu, Q.; Xiao, K.; Wen, L.; Dong, Y.; Xie, G.; Zhang, Z.; Bo, Z.; Jiang, L. A Fluoride-Driven Ionic Gate Based on a 4-Aminophenylboronic Acid-Functionalized Asymmetric Single Nanochannel. *ACS Nano* **2014**, *8*, 12292-12299.

(46) Nie, G.; Sun, Y.; Zhang, F.; Song, M.; Tian, D.; Jiang, L.; Li, H. Fluoride responsive single nanochannel: click fabrication and highly selective sensing in aqueous solution. *Chem. Sci.* **2015**, *6*, 5859-5865.

(47) Xie, G.; Xiao, K.; Zhang, Z.; Kong, X.-Y.; Liu, Q.; Li, P.; Wen, L.; Jiang, L. A Bioinspired Switchable and Tunable Carbonate-Activated Nanofluidic Diode Based on a Single Nanochannel. *Angew. Chem. Int. Ed.* **2015**, *54*, 13664-13668.

(48) Zhang, F.; Ma, J.; Sun, Y.; Boussouar, I.; Tian, D.; Li, H.; Jiang, L. Fabrication of a mercaptoacetic acid pillar[5]arene assembled nanochannel: a biomimetic gate for mercury poisoning. *Chem. Sci.* **2016**, *7*, 3227-3233.

(49) Zhang, F.; Sun, Y.; Tian, D.; Li, H. Chiral Selective Transport of Proteins by Cysteine-Enantiomer-Modified Nanopores. *Angew. Chem. Int. Ed.* **2017**, *56*, 7186-7190.

(50) Wang, R.; Sun, Y.; Zhang, F.; Song, M.; Tian, D.; Li, H. Temperature-Sensitive Artificial Channels through Pillar[5]arene-based Host–Guest Interactions. *Angew. Chem. Int. Ed.* **2017**, *56*, 5294-5298.

(51) Song, M.; Sun, Z.; Han, C.; Tian, D.; Li, H.; Jiang, L. Design and Fabrication of a Biomimetic Nanochannel for Highly Sensitive Arginine Response in Serum Samples. *Chem. Eur. J.* **2014**, *20*, 7987-7993.

(52) Ghidini, E.; Ugozzoli, F.; Ungaro, R.; Harkema, S.; Abu El-Fadl, A.; Reinhoudt, D. N. Complexation of alkali metal cations by conformationally rigid, stereoisomeric calix[4]arene crown ethers: a quantitative evaluation of preorganization. *J. Am. Chem. Soc.* **1990**, *112*, 6979-6985.

(53) Wolbers, M. P.; van Veggel, F. C. J. M.; Heeringa, R. H. M.; Hofstraat, J. W.; Geurts, A. J.; van Hummel, G. J.; Harkema, S.; Reinhoudt, D. N. Biscalix[4]arene Ligands for Dinuclear Lanthanide Ion Complexation. *Liebigs Ann./Recueil* **1997**, *1997*, 2587-2600.

(54) Cervera, J.; Ramirez, P.; Mafe, S.; Stroeve, P. Asymmetric nanopore rectification for ion pumping, electrical power generation, and information processing applications. *Electrochim. Acta* **2011**, *56*, 4504-4511.

(55) Cervera, J.; Schiedt, B.; Neumann, R.; Mafe, S.; Ramirez, P. Ionic Conduction, Rectification, and Selectivity in Single Conical Nanopores. *J. Chem. Phys.* **2006**, *124*, 104706.

(56) Cervera, J.; Schiedt, B.; Ramirez, P. A Poisson/Nernst-Planck model for ionic transport through synthetic conical nanopores. *Europhys. Lett.* **2005**, *71*, 35-41.

(57) Ramirez, P.; Apel, P. Y.; Cervera, J.; Mafe, S. Pore Structure and Function of Synthetic Nanopores with Fixed Charges: Tip Shape and Rectification Properties. *Nanotechnology* **2008**, *19*, 315707.

(58) Ramirez, P.; Gomez, V.; Cervera, J.; Schiedt, B.; Mafe, S. Ion transport and selectivity in nanopores with spatially inhomogeneous fixed charge distributions. *J. Chem. Phys.* **2007**, *126*, 194703.

(59) Siwy, Z. S. Ion-Current Rectification in Nanopores and Nanotubes with Broken Symmetry. *Adv. Funct. Mater.* **2006**, *16*, 735-746.

Figures and Legends

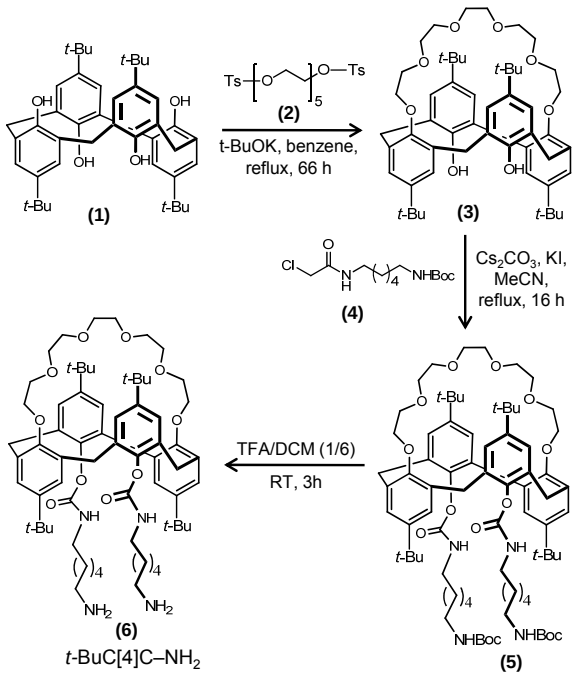

Figure 1. Synthesis of the amine terminated *tert*-butylcalix[4]arene crown (*t*-BuC[4]C–NH_2).

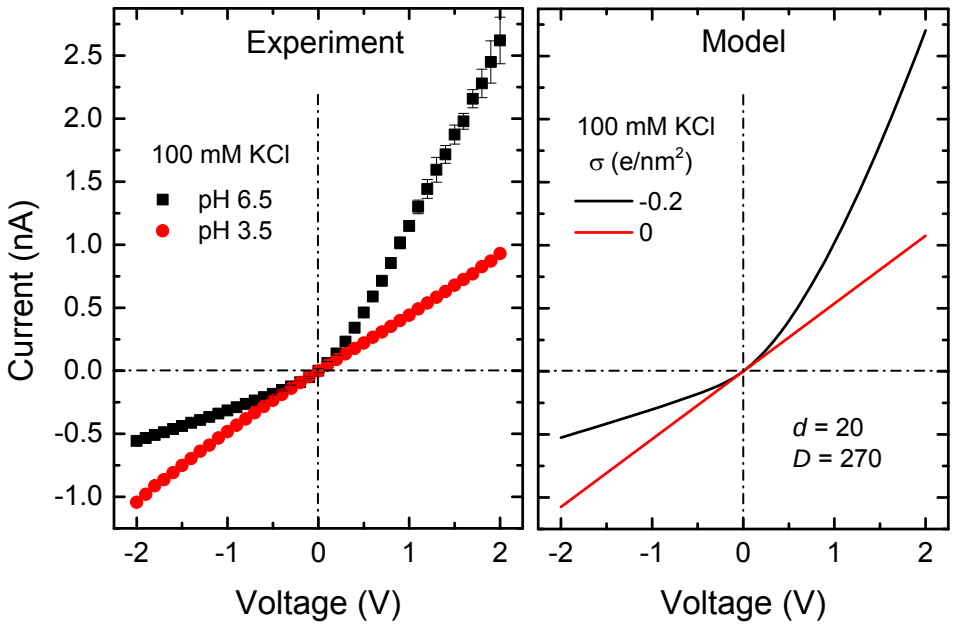

1

2 **Figure 2.** Experimental and theoretical *I–V* characteristics of the as-prepared single
3 conical pore recorded in 100 mM KCl solution at pH 6.5 and 3.5, separately.

4

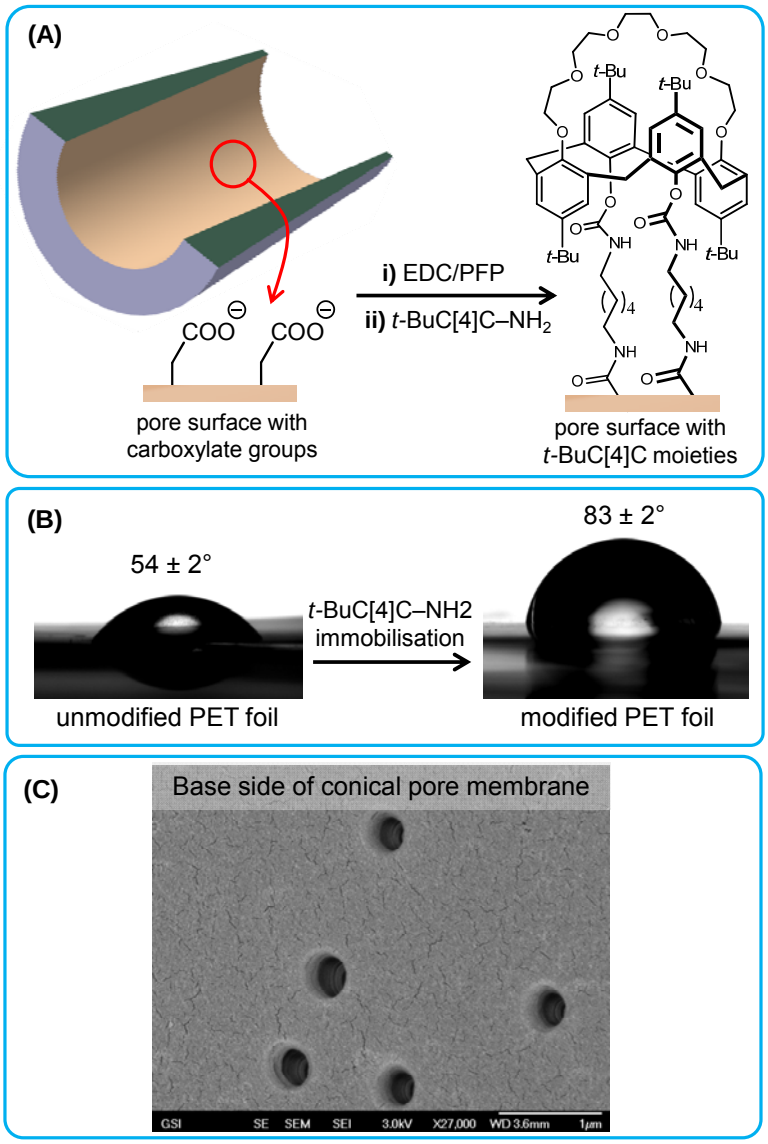

Figure 3. (A) The functionalization of the carboxylic acid groups on the surface of asymmetric nanopore with *tert*-butylcalix[4]arene–crown (*t*-BuC[4]C) moieties via carbodiimide coupling chemistry. (B) The contact angles of an unmodified PET membrane with carboxylic acid groups and a functionalized membrane having *t*-BuC[4]C moieties. (C) FESEM image of the base opening side of the conical pores in a PET membrane having 10^7 pores cm^{-2}.

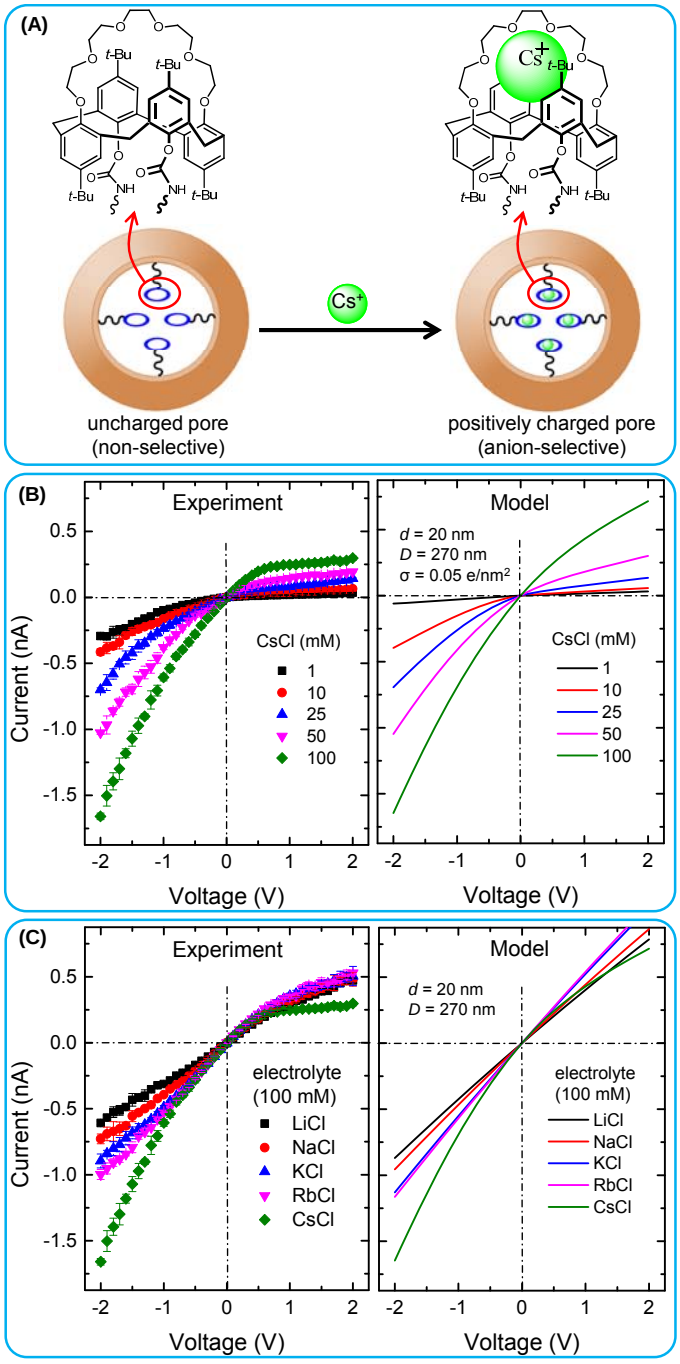

Figure 4. (A) Scheme representing the Cs^+ ion complexation with *t*-BuC[4]C moieties on the pore surface (B) Experimental and theoretical *I–V* characteristics of the modified pore exposed to various concentrations of cesium cation. (C) Experimental and theoretical *I–V* characteristics of the modified pore after the addition of various alkali cations (100 mM, chloride salts) in the electrolyte solution, separately. For CsCl, the estimated value of σ is 0.05 is e/nm^2, while σ is ~ 0.005 e/nm^2 for the other alkali cations.

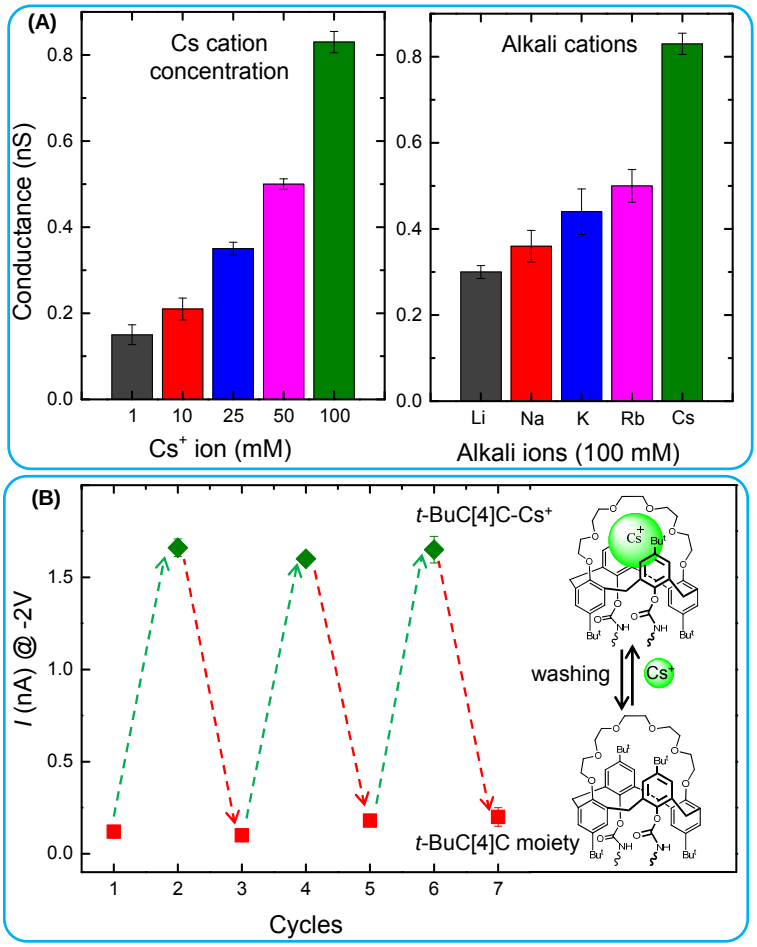

Figure 5. (A) The nanopore conductance measured upon exposure to different Cs cation concentrations and alkali ions obtained from the experimental *I–V* curves shown in Figure 4B and C, respectively. (B) Different cycles representing the changes in the current because of the reversible complexation/decomplexation of Cs^+ ion with the t-BuC[4]C moieties. The current values shown are obtained at a potential of –2 V by exposing the modified pore to electrolyte solutions with no CsCl (red) and 100 mM CsCl (green).

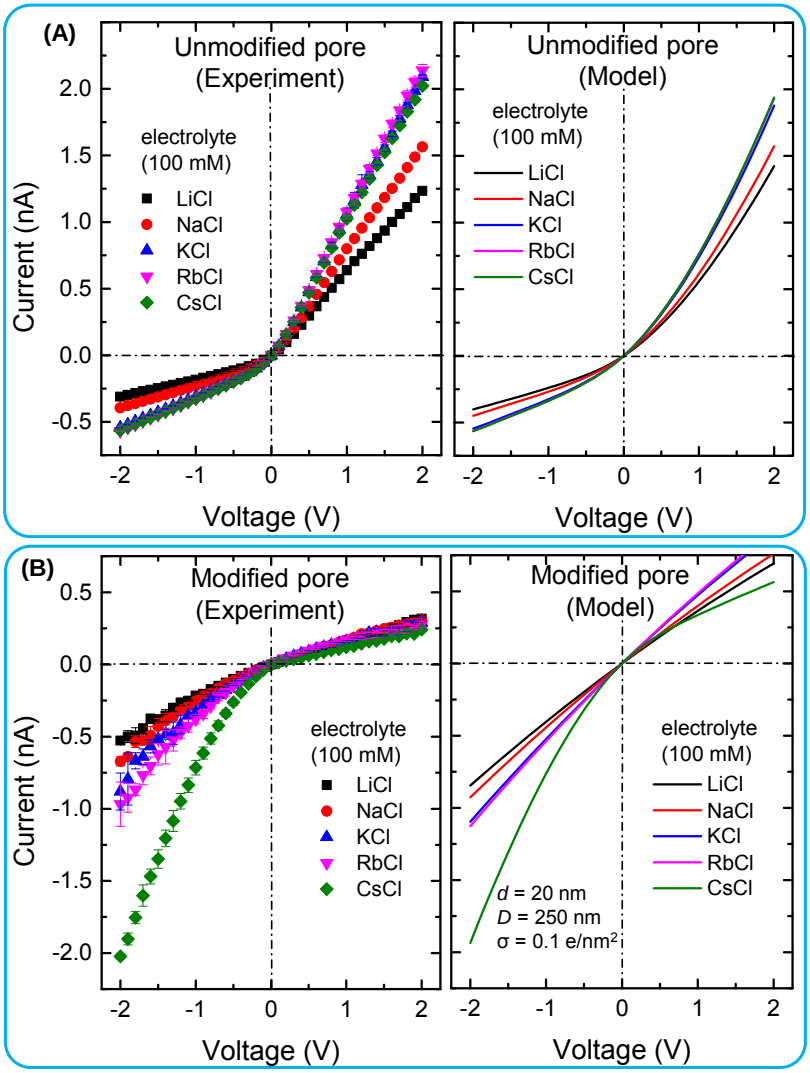

Figure 6. (A) Experimental and theoretical *I–V* characteristics of the unmodified pore on exposure to various alkali cation (100 mM, pH 6.5) solutions, separately. (B) Experimental and theoretical *I–V* characteristics of the modified pore after the addition of various alkali cations (100 mM, chloride salts) in the electrolyte solution, separately. For CsCl, the estimated value of σ is 0.1 is e/nm^2, while σ is ~ 0.01 e/nm^2 for the other alkali cations.

1 **TOC graphics**

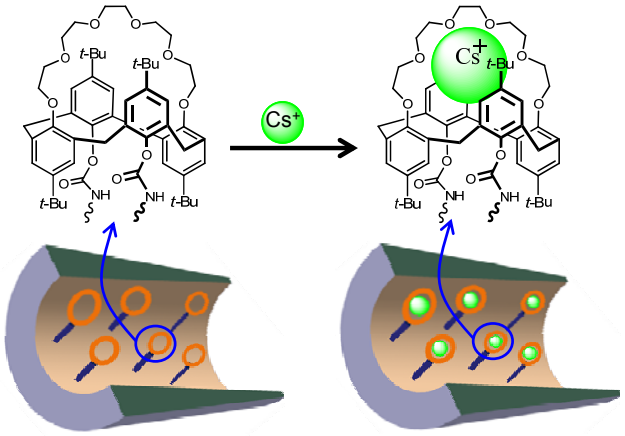

2

3